NANO LETTERS

pubs.acs.org/NanoLett Letter

Spin-Polarized Tunable Photocurrents

Matías Berdakin,*,‖ Esteban A. Rodríguez-Mena,‖ and Luis E. F. Foa Torres*

Cite This: *Nano Lett.* 2021, 21, 3177−3183 Read Online

ACCESS | Metrics & More | Article Recommendations | Supporting Information

ABSTRACT: Harnessing the unique features of topological materials for the development of a new generation of topological based devices is a challenge of paramount importance. Using Floquet scattering theory combined with atomistic models we study the interplay among laser illumination, spin, and topology in a two-dimensional material with spin−orbit coupling. Starting from a topological phase, we show how laser illumination can selectively disrupt the topological edge states depending on their spin. This is manifested by the generation of pure spin photocurrents and spin-polarized charge photocurrents under linearly and circularly polarized laser illumination, respectively. Our results open a path for the generation and control of spin-polarized photocurrents.

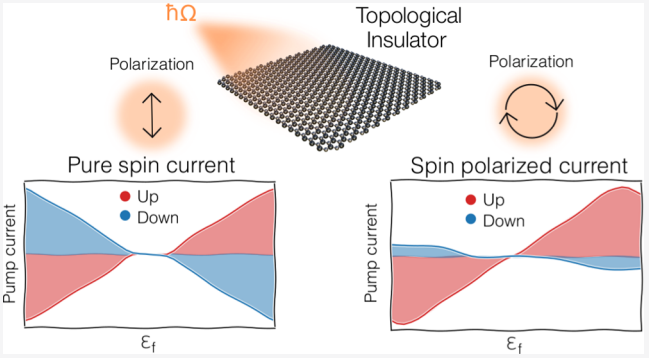

KEYWORDS: *Spin photocurrents, Topological insulators, Two-dimensional materials, Spin−orbit coupling*

INTRODUCTION

The early theoretical proposals[1−4] and the subsequent experimental realization of topological insulators[5,6] have lined up the relentless scientific efforts of an ever growing community in physics, materials science, and chemistry.[7,8] Besides interesting features such as spin-momentum locking,[9] topologically protected states are attractive because, unlike the usual electronic states in solids, they enjoy an intrinsic robustness to perturbations and disorder. But this lack of fragility opens up new challenges for their manipulation. Typical schemes such as surface functionalization[8] are quite ineffective when applied to topological insulators. The difficulty to cleanly turn off the conduction of charge and spin has motivated proposals for a topological field effect transistor[10−13] where the electric field drives a topological transition to a trivial insulating phase, a concept that has been experimentally realized recently.[14]

Another stream of research has been looking to exploit light−matter interaction in materials to control their electrical properties. This includes generating effects such as dichroism,[15,16] a situation where electrons at different valleys absorb left- and right-handed photons differently, which is of much relevance in the context of two-dimensional materials.[17−19] A different approach is aimed at using intense laser illumination to actually change the properties of the material.[20] Indeed, strong illumination has been demonstrated to produce hybrid electron−photon states[21,22] (Floquet-Bloch states) which may present new topological properties[23−25] (see also ref 26) and even exhibit a light-induced Hall effect.[27]

Here, we study laser-illumination on graphene with spin−orbit coupling and a sublattice-symmetry breaking potential. The parameters are fixed so that, in the absence of radiation, the system is in a topologically insulating phase with counter-propagating spin-polarized states protected by time-reversal symmetry. Previous related studies have focused on the rich phase diagram of Floquet topological phases under strong high-frequency radiation ($\hbar\Omega$ larger than the bandwidth)[28] and also considering resonant processes.[29] In contrast to those studies, here we focus on using light to gently disrupt the native topological states. In this regime one might expect an interesting interplay between symmetry breaking (inversion symmetry or time-reversal symmetry, which can be broken or preserved by circular or linearly polarized light), spin−orbit coupling which also intertwined the valley and spin degrees of freedom, and photon-induced processes. Specifically, we show that laser illumination leads to (i) pure spin currents under linearly polarized light and (ii) spin polarized charge currents under circular polarization. In both cases the spin (i) and charge (ii) currents flow even at zero-bias voltage. We rationalize these pumping currents in terms of a selective hybridization of electron-photon states which is enriched by valley and spin-selective selection rules under circular polarization.

HAMILTONIAN MODEL FOR THE FLOQUET−KANE−MELE SYSTEM

Let us now consider the Hamiltonian for graphene with a staggering potential and intrinsic spin−orbit (ISO) interaction:[1]

Received: January 30, 2021
Revised: March 24, 2021
Published: April 5, 2021

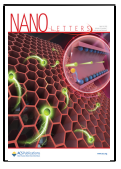

https://doi.org/10.1021/acs.nanolett.1c00420
Nano Lett. 2021, 21, 3177−3183

$$\mathcal{H}_0 = \sum_{i,s_z} E_i c^\dagger_{i,s_z} c_{i,s_z} - \gamma_0 \sum_{\langle i,j\rangle,s_z} c^\dagger_{i,s_z} c_{j,s_z} - \\ - i\gamma_{SO} \sum_{\langle\langle i,j\rangle\rangle,s_z} \nu_{i,j} s_z c^\dagger_{i,s_z} c_{j,s_z} \quad (1)$$

where $c^\dagger_{i,s_z}$ and c_{i,s_z} are the creation and annihilation operators for electrons at the π-orbital on site i with spin up $s_z = 1$ or spin down $s_z = -1$. γ_0 is the nearest-neighbors matrix element, and γ_{SO} is the intrinsic spin−orbit coupling. We set $\gamma_0 = 1$ as our energy scale. $\nu_{i,j}$ is +1 (−1) if the path from j to i is clockwise (anticlockwise), as shown in Figure 1a (right for spin up, left for down). The on-site energies E_i are chosen equal to Δ ($-\Delta$) for the sites on the A (B) sublattice. The single and double brackets denote that the summation is over first or next nearest-neighbors. Although the spin−orbit coupling in bare graphene is too small, the same physics can be realized in other two-dimensional materials such as silicene and germanene[30] where this coupling is stronger.

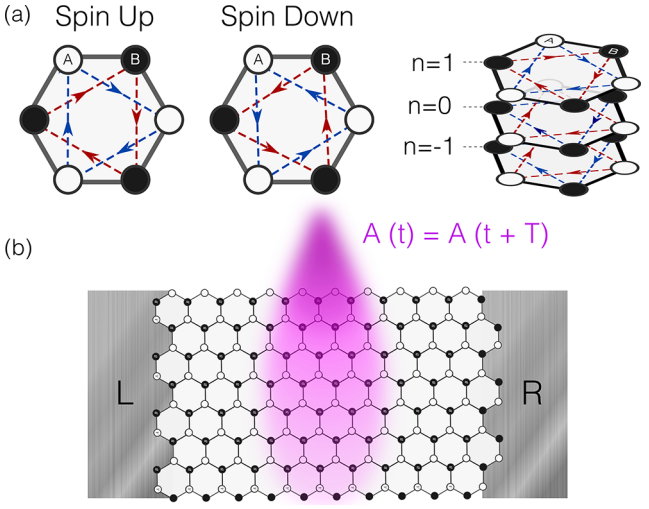

Figure 1. Irradiated Kane−Mele model. In absence of Rashba spin−orbit, one has two decoupled copies of the Haldane model for spin up and down (a, left). Under laser illumination one has the Floquet replica picture representing photon dressed processes (a, right). (b) Scheme of the device considered in the transport setup.

The effect of laser illumination is captured through the Peierls' substitution,[31,32] a time dependent phase in the nearest-neighbors and next-nearest-neighbors matrix elements:

$$\gamma_{i,j}(t) = \gamma^{(0)}_{i,j} \exp\left[i\frac{2\pi}{\Phi_0}\int_{\mathbf{r}_j}^{\mathbf{r}_i} \mathbf{A}(t)\cdot d\mathbf{r}\right] \quad (2)$$

where $\gamma^{(0)}_{i,j}$ are the unperturbed matrix elements as given in eq 1, Φ_0 is the magnetic flux quantum, and $\mathbf{A}(t)$ is the vector potential. For a monochromatic plane wave in the z-direction (perpendicular to the graphene sheet) we consider $\mathbf{A}(t) = A_0 \cos(\Omega t)\hat{x} + A_0 \cos(\Omega t + \phi)\hat{y}$, where Ω is the radiation frequency, A_0 determines the driving amplitude, and $\phi = 0, \pm\pi/2$ controls the polarization linear or left/right-hand polarized, respectively. Right hand polarization is considered whenever we mention circular polarization. The laser strength can be characterized by the dimensionless parameter $z = A_0 a 2\pi/\Phi_0$.

Similar systems were considered before with a few differences: ref 33 studied laser-illuminated transition metal dichalcogenide without the spin−orbit coupling considered here, and refs 29 and 34 studied germanene and silicene in the high-frequency regime while here we focus on frequencies smaller than the bandwidth. Other studies using Floquet theory focused on the topological states induced by light,[35−37] rather than the modification of native topological states considered here. A noteworthy exception is the recent report on the effects of laser illumination on graphene in the the quantum-Hall regime.[38] Throughout this manuscript we use Floquet theory as described in the Supporting Information (see Methods).

QUASIENERGY DISPERSION

Let us start our discussion by analyzing the dispersion relations for a ribbon of laser-illuminated graphene with spin−orbit coupling and a staggering potential. This is shown in Figure 2 for linear (c, d) and circular (e, f) polarization and also without radiation (a, b). Without radiation, when the spin−orbit term dominates over the staggering one, we find the expected topological states bridging the gap. The staggering is responsible for the asymmetry between the valleys, while the overall time-reversal symmetry enforces the mirror symmetry between the plots (when exchanging k by $-k$) for the different spin components. The color scale encodes the contribution of each

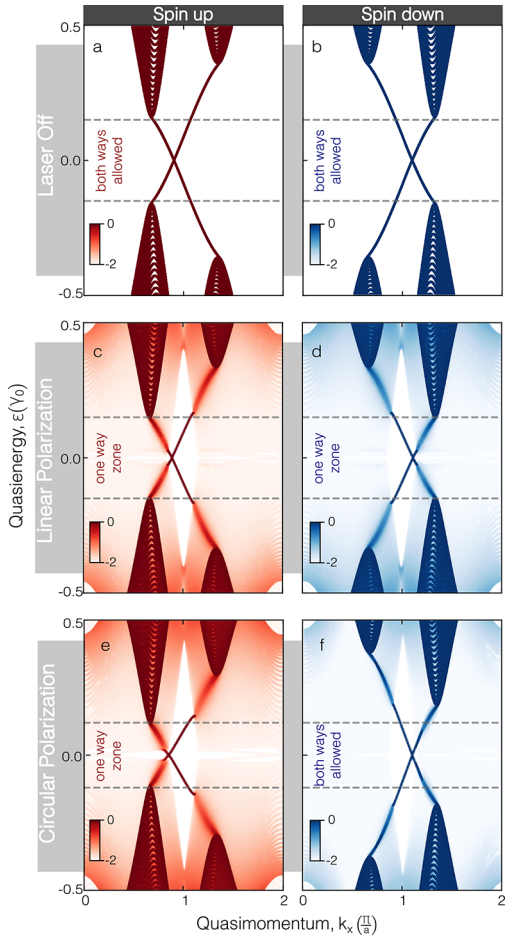

Figure 2. Spin resolved bandstructure of a zigzag ribbon with intrinsic spin−orbit coupling, $W = 100a$ (~25 nm), $\Delta = 0.1$, $\gamma_{SO} = 0.05$, $\hbar\Omega = 1.5$, and $z_x = z_y = 0.15$. Panels (a) and (b) are without irradiation. Panels (c), (d) and (e), (f) are for linear and circular polarized irradiation, respectively. Red (blue) denotes spin up (down). One way or both ways transport regions are highlighted for edge states bridging the bulk gap. The color scale in the bottom shows the time-averaged density of states in log-scale.

https://doi.org/10.1021/acs.nanolett.1c00420
Nano Lett. 2021, 21, 3177−3183

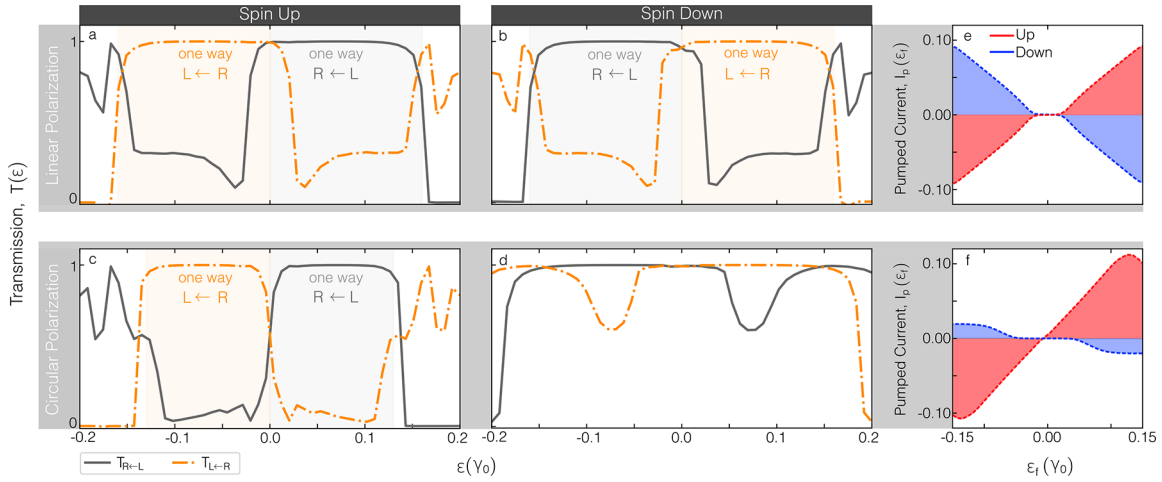

Figure 3. Panels (a)−(d) show the transmission probabilities from left to right and vice versa within the native gap. One-way charge transport is achieved in (a), (b), and (c), while in (d) no one-way effect is witnessed. Panels (e) and (f) present the spin-resolved pump currents obtained for linear and circular polarization. Due to the presence of the pumping currents in the Floquet context, this behavior translates into a zero charge pumping with linear polarization yielding pure spin currents (e) while circular polarization (f) allows for spin polarized charge currents. The former can be tweaked by changing from right-hand to left-hand circular polarization.

state to the time-averaged density of states,[23] which is given by the weight of each state on the reference replica ($n = 0$), which is uniform and equal to unity in the absence of radiation. For linear and circular polarization, the lighter tones (notice the log scale) show the regions with states due to the other replicas (each shifted by $\hbar\Omega$). Radiation will introduce a coupling between the replicas (or, in other words, a coupling between a state with a given k at energy ε and other states at the same k with energy $\varepsilon + n\hbar\Omega$). The effect of such a coupling is the hybridization of the native topological states of this system with the continuum provided by the replicas. In the figure this is evidenced as regions where the lines bridging the gap become blurred (the log scale emphasizes these regions which in normal scale will be hardly visible). Later on, we will see how transport is disrupted due to this hybridization.

Notice that the hybridization with the continuum appearing here is different from that studied in refs 39−41, where the continuum is provided by the states of a second layer in bilayer graphene. In contrast, here this is due to coupling with the continuum in other replicas through photon-assisted processes. Furthermore, spin plays a crucial role in the selection rules as we will highlight later on.

When comparing the results for linear and circular polarization in Figure 2, we find an interesting asymmetry: while with linearly polarized light time reversal symmetry is preserved, circular polarization breaks it. The panels for spin up and down in Figure 2e,f do not mirror each other as when TRS is preserved (panels c and d), and the response is thus expected to be spin-selective. As we will see next, this leads to a deeper selection rule tied to a spin-dependent circular-dichroism effect.

TRANSPORT PROPERTIES

Let us now turn to the transport properties. We consider a two-terminal setup where a central region is being illuminated while the leads remain in equilibrium as sketched in Figure 1b. All the Hamiltonian parameters of the scattering zone and leads are equal. By using Floquet scattering theory as mentioned earlier, we compute the total transmission probabilities as a function of the energy of the incident electrons (ε). Furthermore, we can resolve the contributions of both spin components as shown in Figure 3a−d (readers can find a detailed comparison between Floquet bandstructure and transport signatures in the Supporting Information). While without laser illumination one would expect a perfect and reciprocal transmission equal to unity for energies within the bulk gap, here we see a different picture. First, the left-to-right and right-to-left transmission probabilities differ, as is usual in driven systems with broken symmetries. But interestingly, the response is also highly sensitive to the spin component for circularly polarized light: the results show that one spin component gets stronger scattering (deviations from unity) while the other is less affected. This startling difference in the response for different spins (that is, the difference between Figures 3c,d) begs for an explanation.

The results for the current, which we can resolve in its spin components, are shown in Figure 3e (linear polarization) and Figure 3f (circular polarization). A first fact advanced earlier is that because of the nonreciprocity, there is a photogenerated current that appears even at zero bias voltage. This type of pumped current[42] or photocurrent in this case[43] is intertwined with the symmetry breaking induced by the different terms in the Hamiltonian. While inversion symmetry is broken in all cases (due to the staggering term), for linear polarization TRS is preserved and hence no net charge current can flow in this spinful case. The current per spin component is nonvanishing as shown in Figure 3e, and together both components give a pure spin current.

In contrast, for circular polarization there is a nonvanishing current which turns out to be spin-polarized (see Figure 3f). The polarization depends on the Fermi energy, being almost perfect close to the charge neutrality point and of about 83% at higher/lower energies. The spin-selective nonreciprocity (Figure 3c,d) under circular polarization together with the spin-polarized photocurrents (Figure 3f) are the main numerical results of this paper. Notice that the spin polarization can be inverted by changing the handedness of the laser polarization.

To rationalize the transport results and the quasienergy dispersions we now discuss several points that altogether explain our findings. But first, we need to dig deeper by presenting the different contributions to the total transmissions shown in Figure 3. Indeed, an electron entering the illuminated sample

https://doi.org/10.1021/acs.nanolett.1c00420
Nano Lett. 2021, 21, 3177−3183

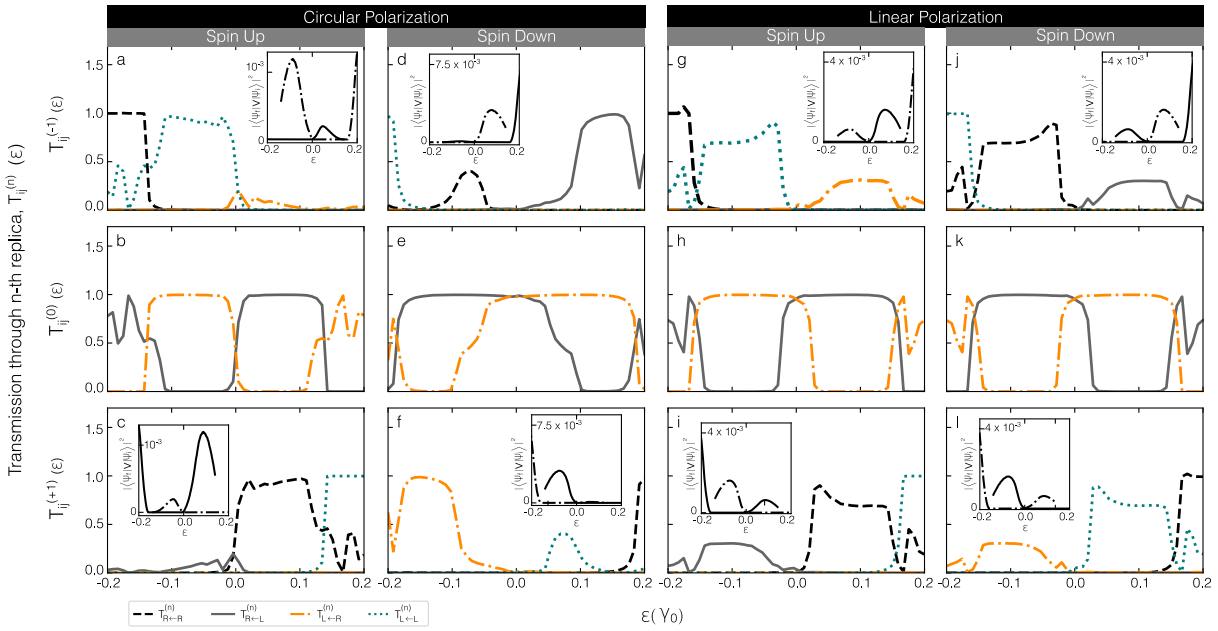

Figure 4. $\mathcal{T}_{ij}^{(n)}(\varepsilon)$ is the transmission probability through a channel mediated by an exchange of n photons with an electron incident with quasienergy ϵ. From panels (a) to (f) is shown $\mathcal{T}_{ij}^{(n)}(\varepsilon)$ under circular polarization, describing the whole process for each spin channel independently. From panels (g) to (l), the same information is depicted for linear polarization. Elastic channels prove to be the main source of transmission, while reflection processes, leading to a one-way transport in regions within the bulk gap, are completely mediated by photon-dressed processes, a distinctive signature of hybridization of the states with the continuum. Insets on each panel quantify the degree of coupling of a native topological state and the bulk bands states induced by higher order replicas. In the insets, solid and dashed lines represent opposite edge chiral states.

with energy ε can exit elastically (without emitting or absorbing a net number of photons) or inelastically. The partial transmissions $\mathcal{T}_{i,j}^{(n)}$ for linear and circular polarization are shown in Figure 4, and a discussion of the role of the inelastic back scattering can be found in the Supporting Information. The insets of Figure 4 show the transition matrix elements between the unperturbed initial and final states. These insets confirm our previous observation that the propagating state with spin down traversing the device is much less disturbed by circularly polarized light than the other.

The following general points explain the observed numerical features:

1. *Generalized symmetry in Floquet space.* The following relation among transmission probabilities is verified in our case:

$$\mathcal{T}_{\beta,\alpha}^{(n)}(\varepsilon) = \mathcal{T}_{\alpha,\beta}^{(-n)}(-\varepsilon) \tag{3}$$

This is enforced by an underlying symmetry in Floquet space:

$$\Gamma\mathcal{H}(\mathbf{k})\Gamma^{\dagger} = -\mathcal{H}(\mathbf{k})^{*} \tag{4}$$

where $\Gamma = \sigma_y K$, K being the complex conjugation operator. This generalized symmetry thus inverts the energy sign while mirroring the space and replica coordinates. This symmetry, which is fulfilled in our device setup, therefore links the transmission probabilities in the different panels of Figures 3 and 4, which also serve as a numerical test of our results. We note that the similar relations have also been used in a different context in Floquet systems.[44]

2. *Spin-selective dichroism effect: a selection rule linking Chern number, circular polarization handedness, and spin.* Under illumination with circularly polarized light we observe a marked transport asymmetry between spin components and also within the same spin subspace when the handedness of the laser polarization changes. The latter is commonly referred to as circular dichroism. The existence of circular dichroism in the presence of both a complex next-nearest-neighbor coupling and a staggering potential for the bulk states has been discussed in ref 45. In that reference, Ghalamkari and coauthors find that there is a selection rule which ties the Chern number of the topological phases found in the Haldane model[46] with a distinctive response to left and right circular polarization.

   In our case, when looking at each spin component separately, our numerical results show that this selection rule persists for a finite system, when the transitions include an edge state and a state in the bulk spectrum. Furthermore, the fact that both spin components are related by the time reversal in $\mathcal{H}_0$ produces an inversion of the circular dichroism when passing from spin up to spin down, since it follows the sign inversion of the spin-resolved Chern number. Here we observe that this inversion of the circular dichroism is also fulfilled for the finite system, a fact which one might intuitively tie in with the bulk-boundary correspondence.

3. *Hybridization of edge states with the continuum provided by a different Floquet replica.* The selection rule stated in point 2 plays a crucial role in establishing the possible light-induced transitions among the electronic states. For Fermi energies within the bulk gap of the sample, thanks to photon-assisted processes, the topological edge states at ε can now transition toward the continuum of states at $\varepsilon + n\hbar\Omega$ (where the system is ungapped). Based on point 2, this hybridization with the states of a different replica is

https://doi.org/10.1021/acs.nanolett.1c00420
Nano Lett. 2021, 21, 3177−3183

expected to be insensitive to the spin for linear polarization but not for circular polarization. This is verified by numerically computing the modulus squared of the matrix element of the perturbation among the initial and final states; see the insets of Figure 4.

For our numerical simulations we employed a general model with staggering potential and spin−orbit coupling compatible with Germanene and Stanene, but we notice that the interplay between the staggering strength, the spin−orbit coupling, and the laser frequency allows for a broad range of materials where the predicted photocurrents could be observed. Indeed, we require a system with with broken inversion symmetry hosting topological states. Within the Kane−Mele model this means that $2\Delta/\gamma_{SO} < 3\sqrt{3}$.[1,46] Furthermore, for the hybridization of the topological states with the continuum of the Floquet replicas to occur, $\hbar\Omega$ needs to be not smaller than the bulk gap of the nonirradiated system and not so large so that there are no continuum states $\hbar\Omega$ above a given energy. Fortunately, these conditions do not impose a restriction within the experimentally relevant regime of laser frequencies spanning from the mid-infrared to the visible range (see Supporting Information). On the other hand, the temperature needed for the experimental realization and the fine-tuning of the irradiation condition will depend on the energy gap of the unperturbed material. The required laser intensities are smaller than those required to observe Floquet−Bloch states, as here we need sufficient coupling with a continuum of states. From our numerics, for typical mid-infrared wavelengths (∼160 meV) we estimate that intensities in the range of 1−10 mW/μm^2 would suffice.

Let us now discuss the influence of Rashba spin−orbit coupling. A Rashba term introduces spin-flip processes, and it is a legitimate source of concern. Our numerical results evidence robustness of the photocurrents against this term (see Supporting Information). This is because the mechanism relies on the existence of topologically protected states in the nonirradiated material, which are originated by intrinsic SOC and which extend to a region of parameters with moderate values of Rashba SOC. Indeed, the topological states are robust against a moderately strong Rashba SOC:[1] for $\lambda_R < 2\sqrt{3}\lambda_{SO}$ (γ_R and γ_{SO} being the strengths of the Rashba and intrinsic spin−orbit coupling terms), the resulting phase diagram is adiabatically connected to the quantum spin-hall phase of the Kane−Mele model. This topological protection means that the matrix element between two topological counter-propagating states at one edge of any perturbation that preserves TRS vanishes. In our case, circular polarization does not preserve TRS, but rather than introducing a matrix element between counter-propagating edge states, leads to a selective hybridization of the edge states with the continuum at an energy differing by $\hbar\Omega$ from them. This is why our results are robust against spin nonconserving terms over a broad range of parameters. Numerical simulations testing the same principle for a model of monolayer $1T'-WTe_2$ (using the model of ref 47) are shown in the Supporting Information.

FINAL REMARKS

Using Floquet scattering theory, we show how laser illumination can selectively disrupt the edge states of a two-dimensional topological insulator depending on their spin. This selectivity, which stems from the interplay between a spin-selective selection rule together with the hybridization of the edge states with the continuum of another Floquet replica, manifests by the generation of pure spin currents and spin-polarized charge photocurrents under linearly and circularly polarized laser illumination, respectively. We emphasize that, in both cases, the spin and charge currents flow even at zero-bias voltage. Furthermore, the direction and spin polarization of these currents can be tuned by changing the incident electronic energy and the handedness of light polarization, thereby providing an experimental handle to control photocurrents. In this sense, given the generality of our model, we expect for the photocurrents predicted here to be experimentally accessible in two-dimensional materials by using laser illumination in the mid-infrared.

ASSOCIATED CONTENT

Supporting Information

The Supporting Information is available free of charge at https://pubs.acs.org/doi/10.1021/acs.nanolett.1c00420.

Discussion of basics of Floquet theory and the generalized Landauer−Büttiker formalism. Also, additional discussions encompassing the relationship between the Floquet band structure and the transport features. Further results supporting the generality of our findings regarding different model parameters, the presence of Rashba SOC, and other materials beyond the Kane and Male model (PDF)

AUTHOR INFORMATION

Corresponding Authors

Matías Berdakin − *INFIQC (CONICET-UNC), Ciudad Universitaria, Pabellón Argentina, 5000 Córdoba, Argentina; Departamento de Química Teórica y Computacional, Fac. de Ciencias Químicas, Universidad Nacional de Córdoba, Ciudad Universitaria, Pabellón Argentina, X5000HUA Córdoba, Argentina;* orcid.org/0000-0002-6517-2765; Email: matiasberdakin@unc.edu.ar

Luis E. F. Foa Torres − *Departamento de Física, Facultad de Ciencias Físicas y Matemáticas, Universidad de Chile, Santiago, Chile*; Email: luis.foatorres@uchile.cl

Author

Esteban A. Rodríguez-Mena − *Departamento de Física, Facultad de Ciencias Físicas y Matemáticas, Universidad de Chile, Santiago, Chile;* orcid.org/0000-0002-7059-8883

Complete contact information is available at: https://pubs.acs.org/10.1021/acs.nanolett.1c00420

Author Contributions

‖(M.B. and E.A.R.-M.) These two authors contributed equally.

Notes

The authors declare no competing financial interest.

ACKNOWLEDGMENTS

E.A.R.-M. acknowledges support from the ANID (Chile) PFCHA, DOCTORADO NACIONAL/2017, under Contract No. 21171229. We are grateful for the support of FondeCyT (Chile) under Grant Number 1170917 and by the EU Horizon 2020 research and innovation program under the Marie-Sklodowska-Curie Grant Agreement No. 873028 (HYDRO-TRONICS Project). L.E.F.F.T. also acknowledges the support of The Abdus Salam International Centre for Theoretical Physics and the Simons Foundation. M.B. acknowledges financial support by Consejo Nacional de Investigaciones Científicas y Técnicas (CONICET) and Secretaría de Ciencia

y Tecnología de la Universidad Nacional de Córdoba (SECYT-UNC).

REFERENCES

(1) Kane, C. L.; Mele, E. J. Quantum Spin Hall Effect in Graphene. *Phys. Rev. Lett.* **2005**, *95*, 226801.
(2) Kane, C. L.; Mele, E. J. ${Z}_{2}$ Topological Order and the Quantum Spin Hall Effect. *Phys. Rev. Lett.* **2005**, *95*, 146802.
(3) Bernevig, B. A.; Hughes, T. L.; Zhang, S.-C. Quantum Spin Hall Effect and Topological Phase Transition in HgTe Quantum Wells. *Science* **2006**, *314*, 1757−1761.
(4) Fu, L.; Kane, C. L. Topological insulators with inversion symmetry. *Phys. Rev. B: Condens. Matter Mater. Phys.* **2007**, *76*, 045302.
(5) König, M.; Wiedmann, S.; Brüne, C.; Roth, A.; Buhmann, H.; Molenkamp, L. W.; Qi, X.-L.; Zhang, S.-C. Quantum Spin Hall Insulator State in HgTe Quantum Wells. *Science* **2007**, *318*, 766−770.
(6) Hsieh, D.; Qian, D.; Wray, L.; Xia, Y.; Hor, Y. S.; Cava, R. J.; Hasan, M. Z. A topological Dirac insulator in a quantum spin Hall phase. *Nature* **2008**, *452*, 970−974.
(7) Ren, Y.; Qiao, Z.; Niu, Q. Topological phases in two-dimensional materials: a review. *Rep. Prog. Phys.* **2016**, *79*, 066501.
(8) Kong, D.; Cui, Y. Opportunities in chemistry and materials science for topological insulators and their nanostructures. *Nat. Chem.* **2011**, *3*, 845−849.
(9) Ortmann, F.; Roche, S.; Valenzuela, S. O.; Molenkamp, L. W. *Topological Insulators: Fundamentals and Perspectives*; Wiley-VCH: Weinheim, Germany, 2015.
(10) Qian, X.; Liu, J.; Fu, L.; Li, J. Quantum spin Hall effect in two-dimensional transition metal dichalcogenides. *Science* **2014**, *346*, 1344−1347.
(11) Liu, J.; Hsieh, T. H.; Wei, P.; Duan, W.; Moodera, J.; Fu, L. Spin-filtered edge states with an electrically tunable gap in a two-dimensional topological crystalline insulator. *Nat. Mater.* **2014**, *13*, 178−183.
(12) Pan, H.; Wu, M.; Liu, Y.; Yang, S. A. Electric control of topological phase transitions in Dirac semimetal thin films. *Sci. Rep.* **2015**, *5*, 14639.
(13) Vandenberghe, W. G.; Fischetti, M. V. Imperfect two-dimensional topological insulator field-effect transistors. *Nat. Commun.* **2017**, *8*, 14184.
(14) Collins, J. L.; Tadich, A.; Wu, W.; Gomes, L. C.; Rodrigues, J. N. B.; Liu, C.; Hellerstedt, J.; Ryu, H.; Tang, S.; Mo, S.-K.; Adam, S.; Yang, S. A.; Fuhrer, M. S.; Edmonds, M. T. Electric-field-tuned topological phase transition in ultrathin Na 3 Bi. *Nature* **2018**, *564*, 390−394.
(15) Xiao, D.; Yao, W.; Niu, Q. Valley-Contrasting Physics in Graphene: Magnetic Moment and Topological Transport. *Phys. Rev. Lett.* **2007**, *99*, 236809.
(16) Cao, T.; Wang, G.; Han, W.; Ye, H.; Zhu, C.; Shi, J.; Niu, Q.; Tan, P.; Wang, E.; Liu, B.; Feng, J. Valley-selective circular dichroism of monolayer molybdenum disulphide. *Nat. Commun.* **2012**, *3*, 887.
(17) Sie, E. J.; McIver, J. W.; Lee, Y.-H.; Fu, L.; Kong, J.; Gedik, N. Valley-selective optical Stark effect in monolayer WS_2. *Nat. Mater.* **2015**, *14*, 290−294.
(18) Zeng, H.; Dai, J.; Yao, W.; Xiao, D.; Cui, X. Valley polarization in MoS 2 monolayers by optical pumping. *Nat. Nanotechnol.* **2012**, *7*, 490−493.
(19) Zhang, L.; Gong, K.; Chen, J.; Liu, L.; Zhu, Y.; Xiao, D.; Guo, H. Generation and transport of valley-polarized current in transition-metal dichalcogenides. *Phys. Rev. B: Condens. Matter Mater. Phys.* **2014**, *90*, 195428.
(20) Quantum phases on demand. *Nat. Phys.* **2020**, *16*, 1; DOI: 10.1038/s41567-019-0781-4.
(21) Wang, Y. H.; Steinberg, H.; Jarillo-Herrero, P.; Gedik, N. Observation of Floquet-Bloch States on the Surface of a Topological Insulator. *Science* **2013**, *342*, 453−457.
(22) Mahmood, F.; Chan, C.-K.; Alpichshev, Z.; Gardner, D.; Lee, Y.; Lee, P. A.; Gedik, N. Selective scattering between Floquet-Bloch and Volkov states in a topological insulator. *Nat. Phys.* **2016**, *12*, 306−310.
(23) Oka, T.; Aoki, H. Photovoltaic Hall effect in graphene. *Phys. Rev. B: Condens. Matter Mater. Phys.* **2009**, *79*, 081406.
(24) Lindner, N. H.; Refael, G.; Galitski, V. Floquet topological insulator in semiconductor quantum wells. *Nat. Phys.* **2011**, *7*, 490−495.
(25) Rudner, M. S.; Lindner, N. H. Band structure engineering and non-equilibrium dynamics in Floquet topological insulators. *Nature Reviews Physics* **2020**, *2*, 229−244.
(26) Giustino, F.; Lee, J. H.; Trier, F.; Bibes, M.; Winter, S. M.; Valentí, R.; Son, Y.-W.; Taillefer, L.; Heil, C.; Figueroa, A. I.; Plaçais, B.; Wu, Q.; Yazyev, O. V.; Bakkers, E. P. A. M.; Nygård, J.; Forn- Díaz, P.; De Franceschi, S.; McIver, J. W.; Torres, L. E. F. F.; Low, T.; Kumar, A.; Galceran, R.; Valenzuela, S. O.; Costache, M. V.; Manchon, A.; Kim, E.-A.; Schleder, G. R.; Fazzio, A.; Roche, S.; et al. The 2021 quantum materials roadmap. *J. Phys. Mater.* **2020**, *3*, 042006.
(27) McIver, J. W.; Schulte, B.; Stein, F.-U.; Matsuyama, T.; Jotzu, G.; Meier, G.; Cavalleri, A. Light-induced anomalous Hall effect in graphene. *Nat. Phys.* **2020**, *16*, 38−41.
(28) Ezawa, M. Photoinduced Topological Phase Transition and a Single Dirac-Cone State in Silicene. *Phys. Rev. Lett.* **2013**, *110*, 026603.
(29) López, A.; Scholz, A.; Santos, B.; Schliemann, J. Photoinduced pseudospin effects in silicene beyond the off-resonant condition. *Phys. Rev. B: Condens. Matter Mater. Phys.* **2015**, *91*, 125105.
(30) Ezawa, M. Monolayer Topological Insulators: Silicene, Germanene, and Stanene. *J. Phys. Soc. Jpn.* **2015**, *84*, 121003.
(31) Calvo, H. L.; Pastawski, H. M.; Roche, S.; Foa Torres, L. E. F. Tuning laser-induced band gaps in graphene. *Appl. Phys. Lett.* **2011**, *98*, 232103−3.
(32) Calvo, H. L.; Perez-Piskunow, P. M.; Pastawski, H. M.; Roche, S.; Foa Torres, L. E. F. Non-perturbative effects of laser illumination on the electrical properties of graphene nanoribbons. *J. Phys.: Condens. Matter* **2013**, *25*, 144202.
(33) Huamán, A.; Usaj, G. Floquet spectrum and two-terminal conductance of a transition-metal dichalcogenide ribbon under a circularly polarized laser field. *Phys. Rev. B: Condens. Matter Mater. Phys.* **2019**, *99*, 075423.
(34) Tahir, M.; Zhang, Q. Y.; Schwingenschlögl, U. Floquet edge states in germanene nanoribbons. *Sci. Rep.* **2016**, *6*, 31821.
(35) Bajpai, U.; Ku, M. J. H.; Nikolić, B. K. Robustness of quantized transport through edge states of finite length: Imaging current density in Floquet topological versus quantum spin and anomalous Hall insulators. *Phys. Rev. Research* **2020**, *2*, 033438.
(36) Farrell, A.; Pereg-Barnea, T. Photon-Inhibited Topological Transport in Quantum Well Heterostructures. *Phys. Rev. Lett.* **2015**, *115*, 106403.
(37) Sato, S. A.; Tang, P.; Sentef, M. A.; Giovannini, U. D.; Hübener, H.; Rubio, A. Light-induced anomalous Hall effect in massless Dirac fermion systems and topological insulators with dissipation. *New J. Phys.* **2019**, *21*, 093005.
(38) Huamán, A.; Foa Torres, L. E. F.; Balseiro, C. A.; Usaj, G. Quantum Hall edge states under periodic driving: A Floquet induced chirality switch. *Phys. Rev. Research* **2021**, *3*, 013201.
(39) Foa Torres, L. E. F.; Dal Lago, V.; Suárez Morell, E. Crafting zero-bias one-way transport of charge and spin. *Phys. Rev. B: Condens. Matter Mater. Phys.* **2016**, *93*, 075438.
(40) Dal Lago, V.; Suárez Morell, E.; Foa Torres, L. E. F. One-way transport in laser-illuminated bilayer graphene: A Floquet isolator. *Phys. Rev. B: Condens. Matter Mater. Phys.* **2017**, *96*, 235409.
(41) Berdakin, M.; Barrios Vargas, J. E.; Foa Torres, L. E. F. Directional control of charge and valley currents in a graphene-based device. *Phys. Chem. Chem. Phys.* **2018**, *20*, 28720−28725.
(42) Moskalets, M.; Büttiker, M. Floquet scattering theory of quantum pumps. *Phys. Rev. B: Condens. Matter Mater. Phys.* **2002**, *66*, 205320.
(43) Bajpai, U.; Popescu, B. S.; Plecháč, P.; Nikolić, B. K.; Torres, L. E. F. F.; Ishizuka, H.; Nagaosa, N. Spatio-temporal dynamics of shift current quantum pumping by femtosecond light pulse. *Journal of Physics: Materials* **2019**, *2*, 025004.
(44) Balabanov, O.; Johannesson, H. Transport signatures of symmetry protection in 1D Floquet topological insulators. *J. Phys.: Condens. Matter* **2019**, *32*, 015503.

https://doi.org/10.1021/acs.nanolett.1c00420
Nano Lett. 2021, 21, 3177−3183

(45) Ghalamkari, K.; Tatsumi, Y.; Saito, R. Perfect Circular Dichroism in the Haldane Model. *J. Phys. Soc. Jpn.* **2018**, *87*, 063708.
(46) Haldane, F. D. M. Model for a Quantum Hall Effect without Landau Levels: Condensed-Matter Realization of the "Parity Anomaly. *Phys. Rev. Lett.* **1988**, *61*, 2015−2018.
(47) Lau, A.; Ray, R.; Varjas, D.; Akhmerov, A. R. Influence of lattice termination on the edge states of the quantum spin Hall insulator monolayer 1T WTe2. *Phys. Rev. Materials* **2019**, *3*, 054206.

https://doi.org/10.1021/acs.nanolett.1c00420
Nano Lett. 2021, 21, 3177−3183